

Supplementary Materials

Superior Strength and Highly Thermoconductive Cellulose/ Boron Nitride Film by Stretch-induced Alignment

Hu Tu,^{1,3,#} Kang Xie,^{2,#} Xinghuan Lin,¹ Ruquan Zhang,³ Feng Chen,² Qiang Fu,^{2,*} Bo Duan,^{1,*} Lina Zhang¹

¹ College of Chemistry and Molecular Sciences, Hubei Engineering Center of Natural Polymer-based Medical Materials and Key Laboratory of Biomedical Polymers of Ministry of Education, Wuhan University, Wuhan 430072, China

² College of Polymer Science and Engineering, Sichuan University, Chengdu 610065, China

³ State Key Laboratory of New Textile Materials and Advanced Processing Technologies, Wuhan Textile University, Wuhan 430200, China

Hu Tu and Kang Xie contributed equally to this work.

Correspondence to:

qiangfu@scu.edu.cn (Q. Fu), bo_duan@whu.edu.cn (B. Duan)

Table S1 the components of different cellulose/BN-OH solution

Solution	BNNS-OH percent (%)	LiOH/urea solvent (g)	Cellulose (g)	BNNS- OH (g)
cellulose	0	100	5.5	0
cellulose/10%BNNS-OH	10	100	5.5	0.55
cellulose/30%BNNS-OH	30	100	5.5	1.65
cellulose/50%BNNS-OH	50	100	5.5	2.75
cellulose/70%BNNS-OH	70	100	5.5	3.85

Table S2 The atomic percent of cellulose/BNNS-OH films with various ratios of BNNS-OH from EDS results.

Elements (%) Samples	C	O	B	N
cellulose-1.0	80.02	19.98	0	0
10%BN-1.0	67.31	13.29	11.22	8.19
30%BN-1.0	55.38	15.99	15.51	13.12
50%BN-1.0	49.58	8.63	21.90	19.90
70%BN-1.0	44.48	6.93	27.44	21.14

Table S3 The comparison of (002) and (100) peaks intensities with 50%BN-1.0, 50%BN-2.0 and 50%BN-3.0 from the XRD results.

Samples	50%BN-1.0	50%BN-2.0	50%BN-3.0
$I_{(002)}$	76865	82155	108905
$I_{(100)}$	1030	920	1100
$I_{(002)}/I_{(100)}$	74.6	89.3	99.0

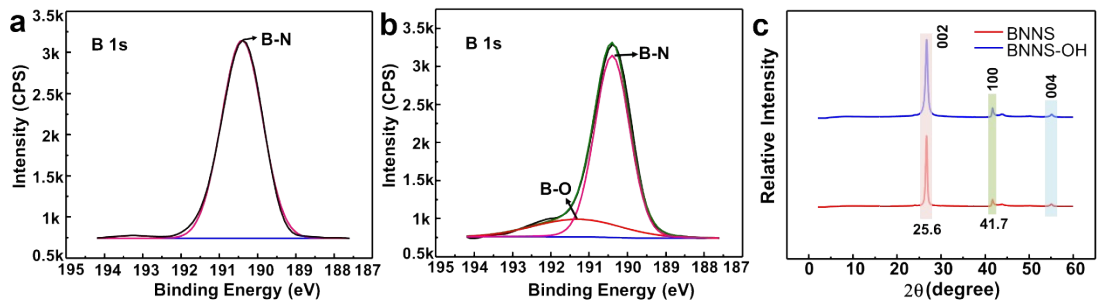


Fig. S1 XPS B1s spectrum of BNNS (a) and BNNS-OH (b). The XRD patterns of BNNS and BNNS-OH (c).



Fig. S2 BNNS and BNNS-OH dispersed in alkali/urea solution for 24h.

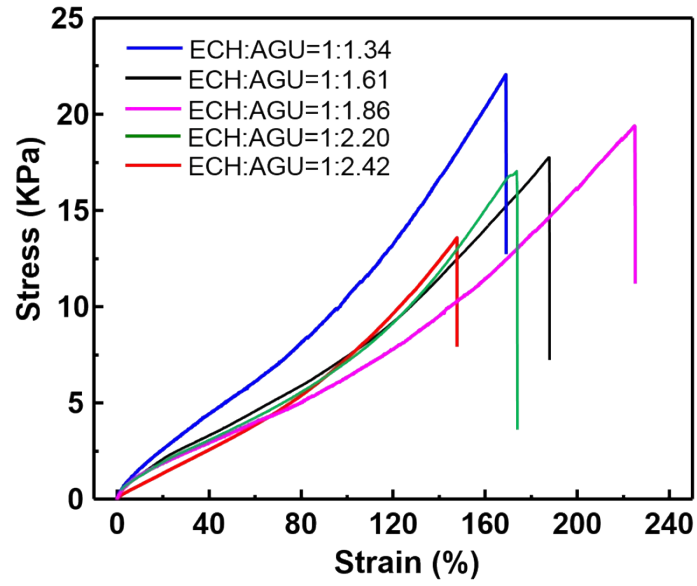


Fig. S3 Tensile stress–strain curves of chemical crosslinked hydrogels with differential dosage of chemical crosslinker (ECH).

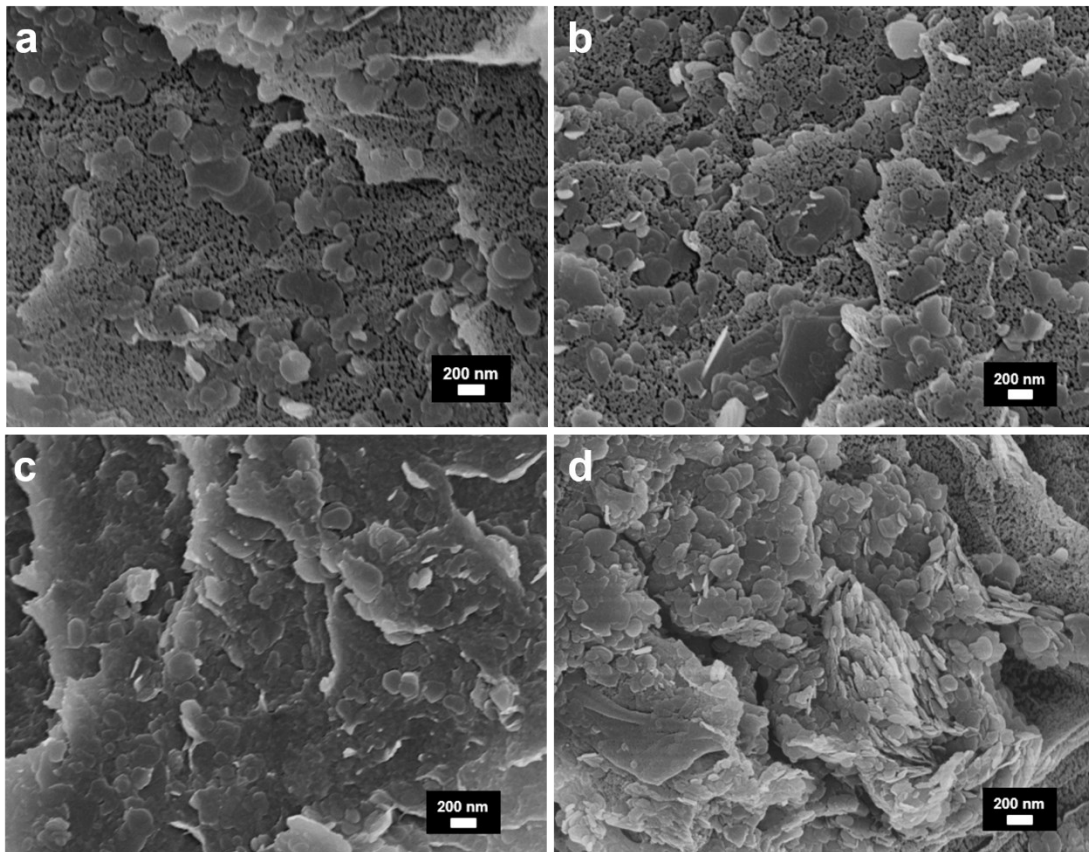


Fig. S4 SEM images of 10%BN-1.0 (a), 30%BN-1.0 (b), 50%BN-1.0 (c) and 70%BN-1.0 (d).

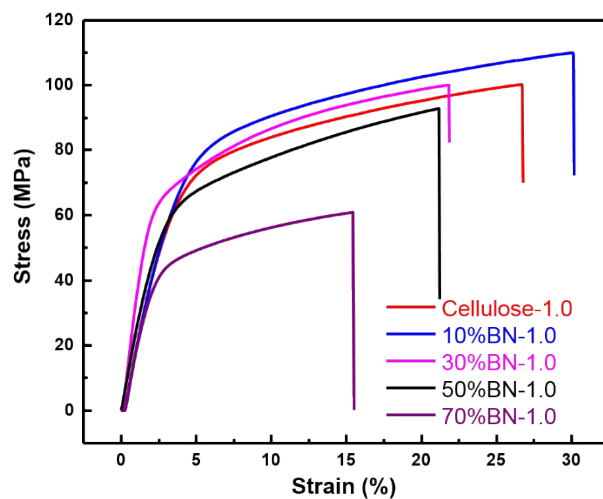


Fig. S5 Stress–strain curves of the dual-cross-linked cellulose films loaded with various ratios of BNNS-OH.

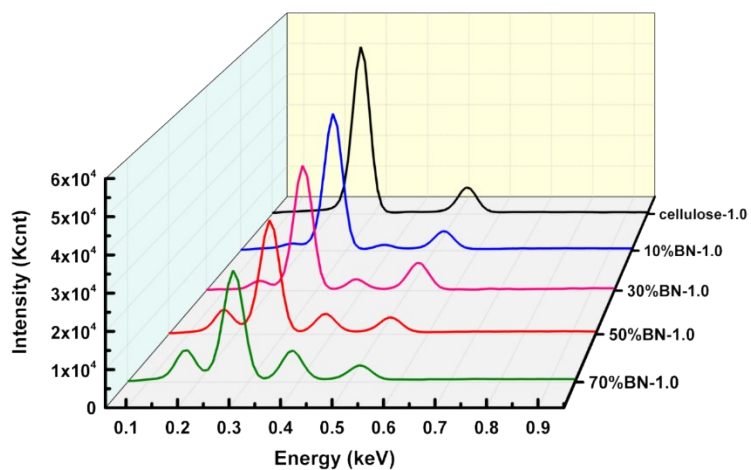


Fig. S6 EDS spectra of cellulose/BNNS-OH films with various ratios of BNNS-OH.

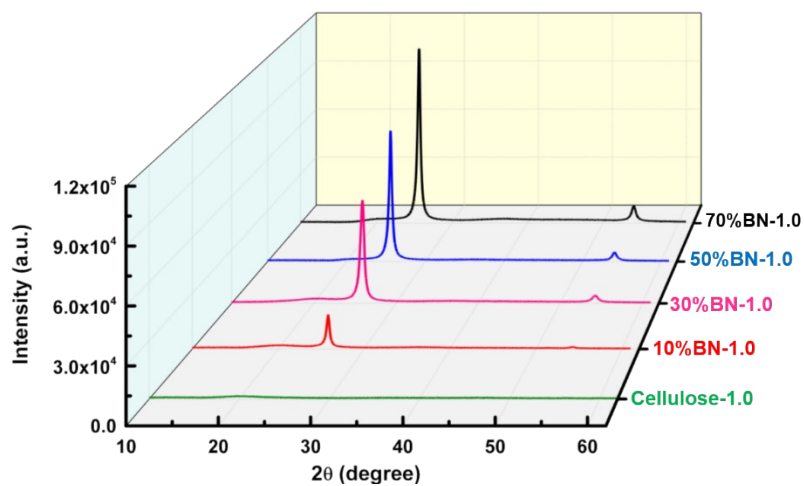


Fig. S7 The XRD patterns of cellulose/BNNS-OH films with various ratios of BN-OH.

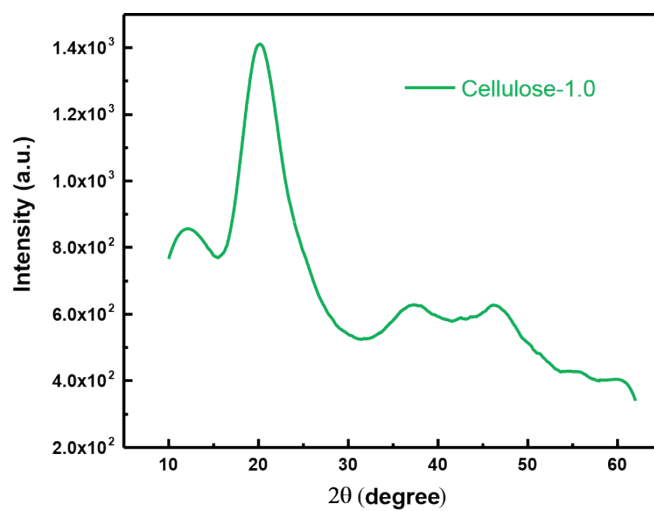


Fig. S8 The XRD patterns of cellulose-1.0.

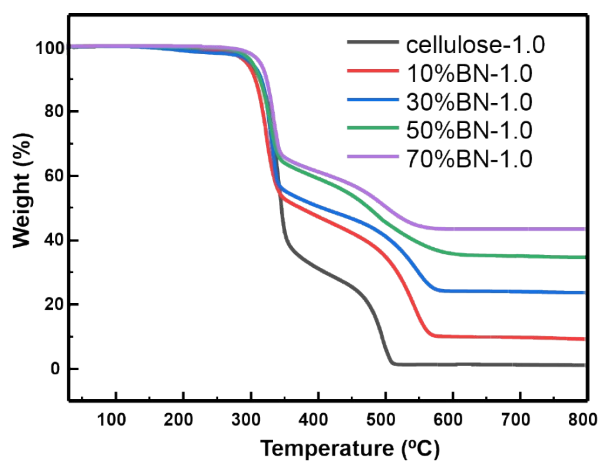


Fig. S9 The TGA results of cellulose/BNNS-OH films with various ratios of BNNS-OH.

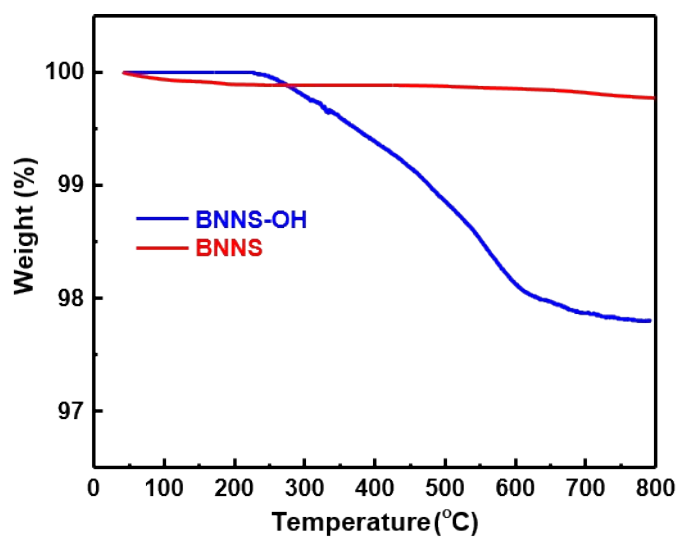
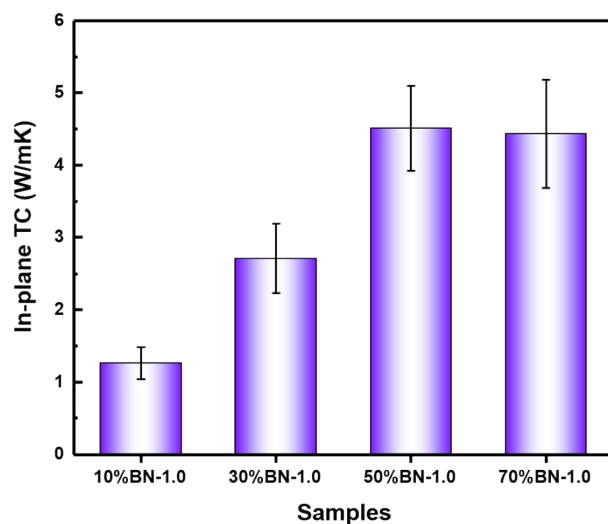


Fig. S10 The TGA results of BNNS and BNNS-OH.



Figur. S11 The in-plane thermal conductivities (TC) of the cellulose/BNNS-OH films with different BNNS-OH content.

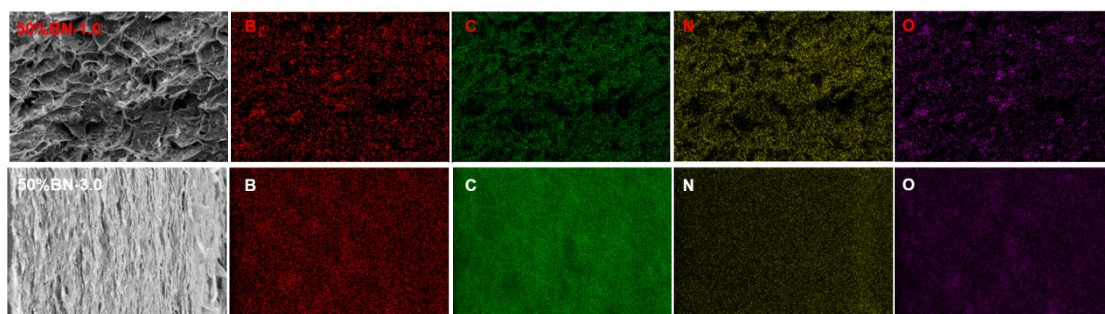


Fig. S12 The EDS mapping patterns of 50%BN-1.0 and 50%BN-3.0.

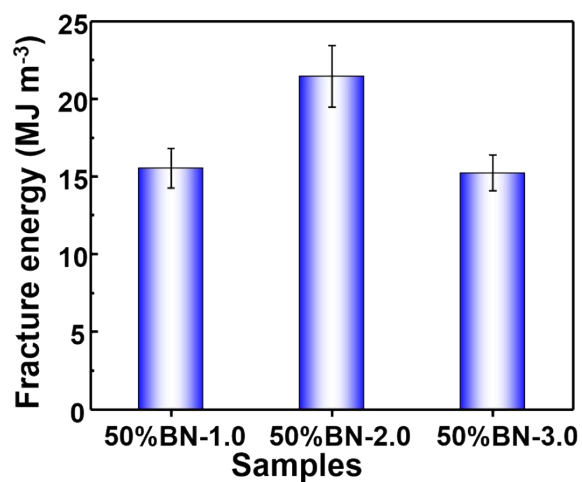


Fig. S13 The fracture energy of 50%BN-1.0, 50%BN-2.0 and 50%BN-3.0

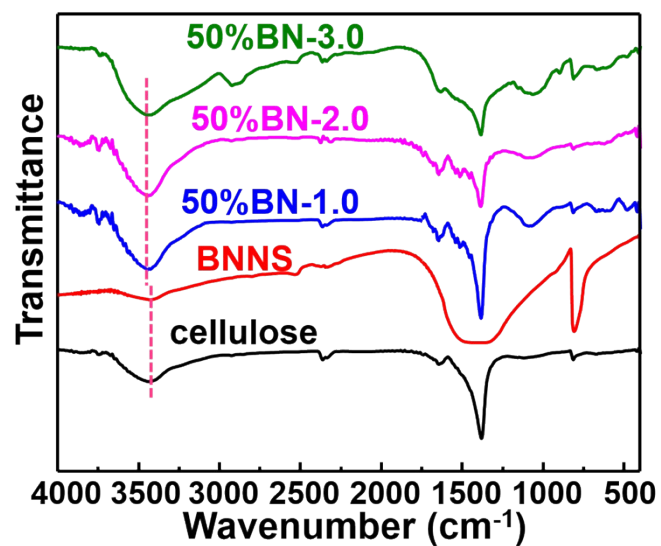


Fig. S14 FT-IR spectra of various samples.

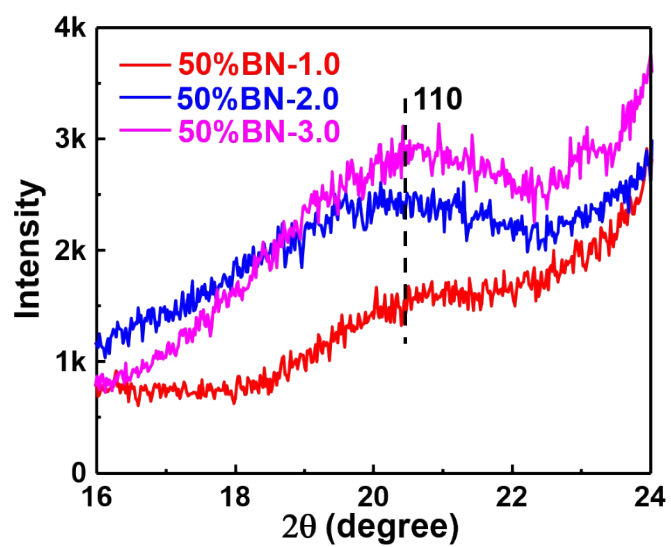


Fig. S15 The XRD patterns of 50%BN-1.0, 50%BN-2.0 and 50%BN-3.0 from Fig. 3f.

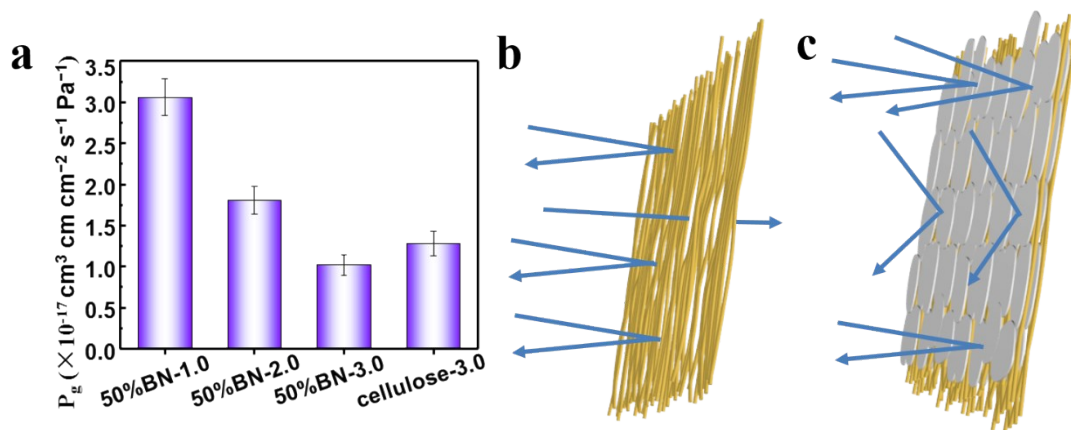


Fig. S16 The oxygen permeability of various samples (a). The schematic diagram of the gas barrier properties of cellulose-3.0 (b) and 50%BN-3.0 (c).



Fig. S17 The photographs of the signal intensities of the mobile phone coated with the commercial graphene film.